Supporting Information

Topography, spike dynamics and nanomechanics of individual native SARS-CoV-2 virions

Bálint Kiss[1#], Zoltán Kis[2,3#], Bernadett Pályi[2], Miklós S.Z. Kellermayer[1]*

[1]Department of Biophysics and Radiation Biology, Semmelweis University, Tűzoltó str. 37-47., Budapest, H-1094 Hungary

[2]National Biosafety Laboratory, National Public Health Center, Albert Flórián Rd 2-6., Budapest, H-1097 Hungary

[3]Department of Medical Microbiology, Semmelweis University, Nagyvárad Sq. 4., H-1089 Hungary

[#]These authors contributed equally

*to whom correspondence may be addressed at: kellermayer.miklos@med.semmelweis-univ.hu

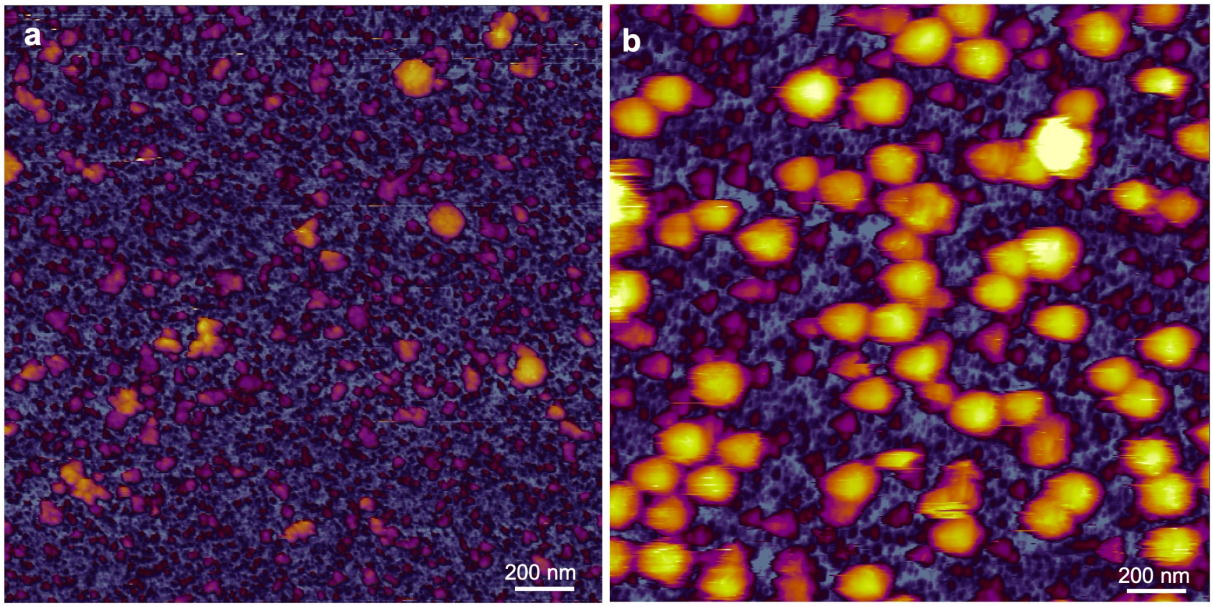

Fig. S1. Effect of using monoclonal anti-spike antibody for affinity-enhanced surface binding of SARS-Cov-2 virions. **a.** AFM image of an overview (2 x 2 µm) sample area where protein G and the anti-spike protein antibody were omitted, and the virus sample was directly loaded onto a mica surface coated with poly-L-lysine and glutaraldehyde. **b.** AFM image of an overview (2 x 2 µm) sample area where the viruses were captured by the anti-spike protein antibody on the substrate surface. Binding was amplified by nearly two orders of magnitude.

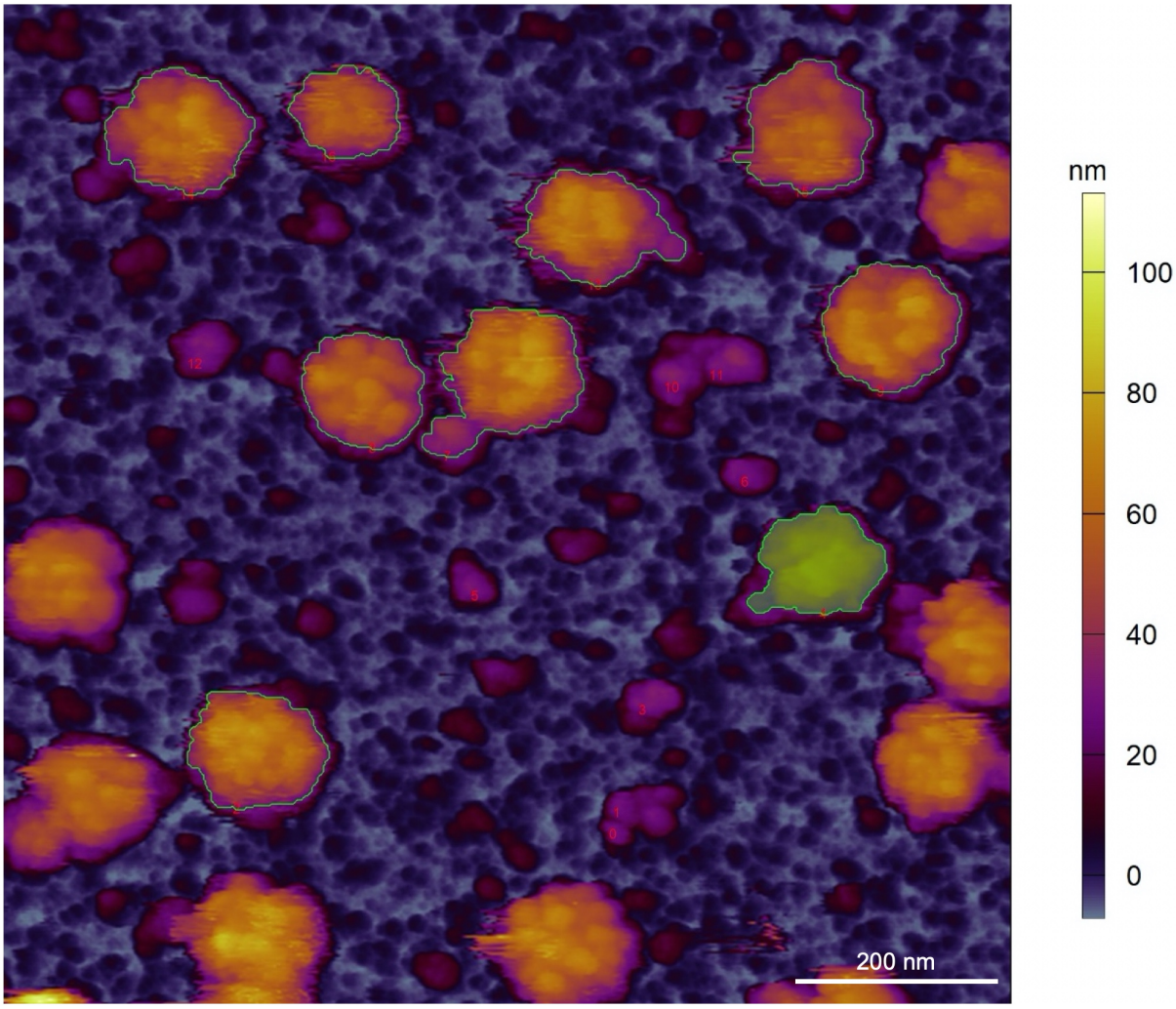

Fig. S2. Particle analysis carried out in AFM images of SARS-CoV-2 virions. Green line surrounding particles shows the contour at the average half peak height, which defines the border of the analyzed particles. One such particle fit for analysis is filled with green colour.

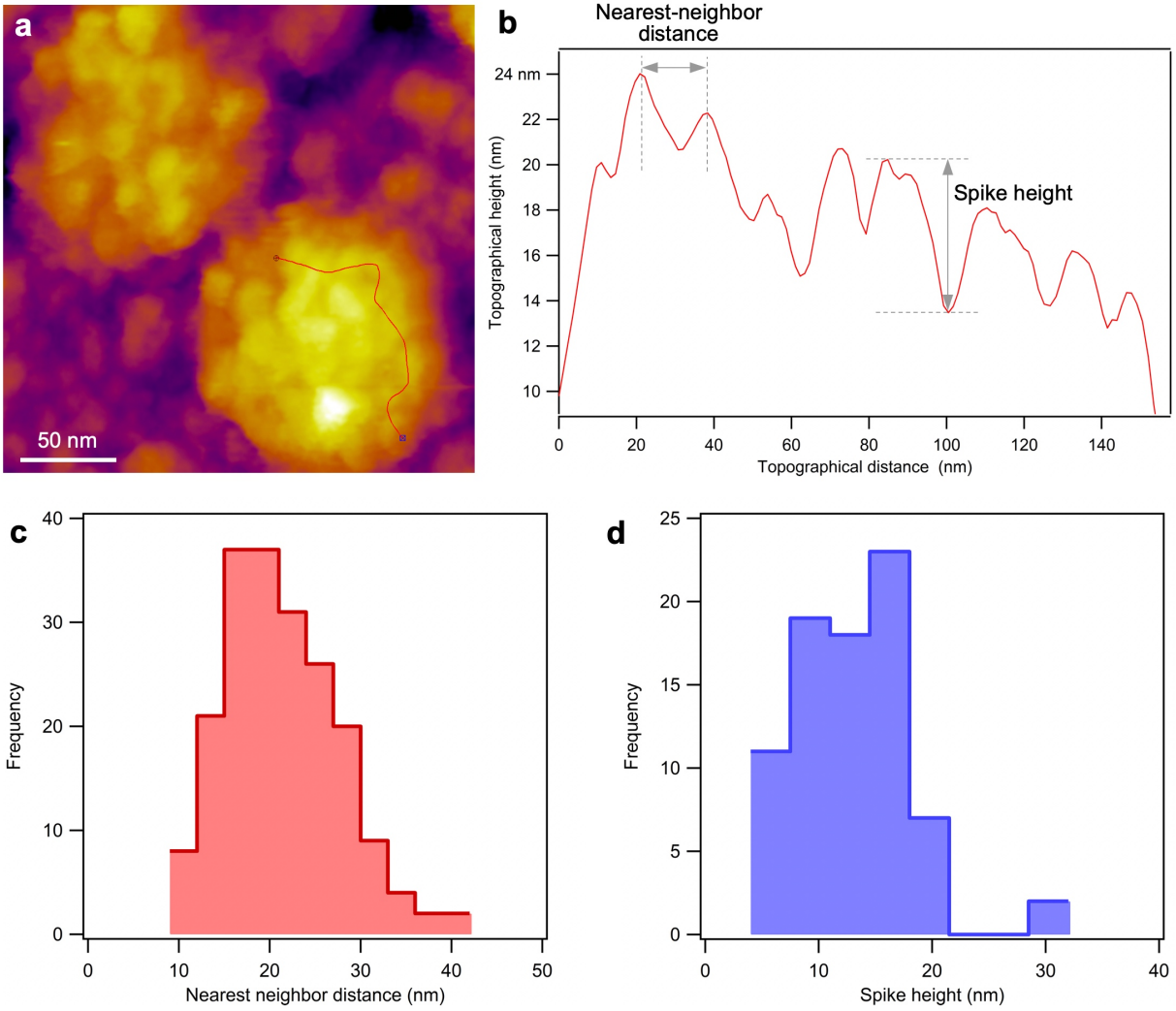

Fig. S3. Measurement of the nearest-neighbor distance between and the height of S trimers. **a.** AFM image of two SARS-CoV-2 virions fixed with glutaraldehyde (5%). Red line indicates the path, drawn approximately in coronal plane, along which the topographical height was measured. **b.** Topographical profile plot of the virion along the line indicated in **a**. Nearest-neighbor distance was obtained by measuring the distance between subsequent peaks. Spike height was obtained by measuring the distance, along the height axis, between a peak and the immediately following valley. Height was measured only for spikes with a large enough valley so as to increase the probability of the AFM tip reaching the envelope surface. **c.** Distribution of the nearest neighbor distance between spikes (n=197), the wide range of which reflects positional disorder (range=31 nm). **d.** Distribution of the spike height (n=80), the wide range of which reflects flexural disorder (range=26.7 nm).

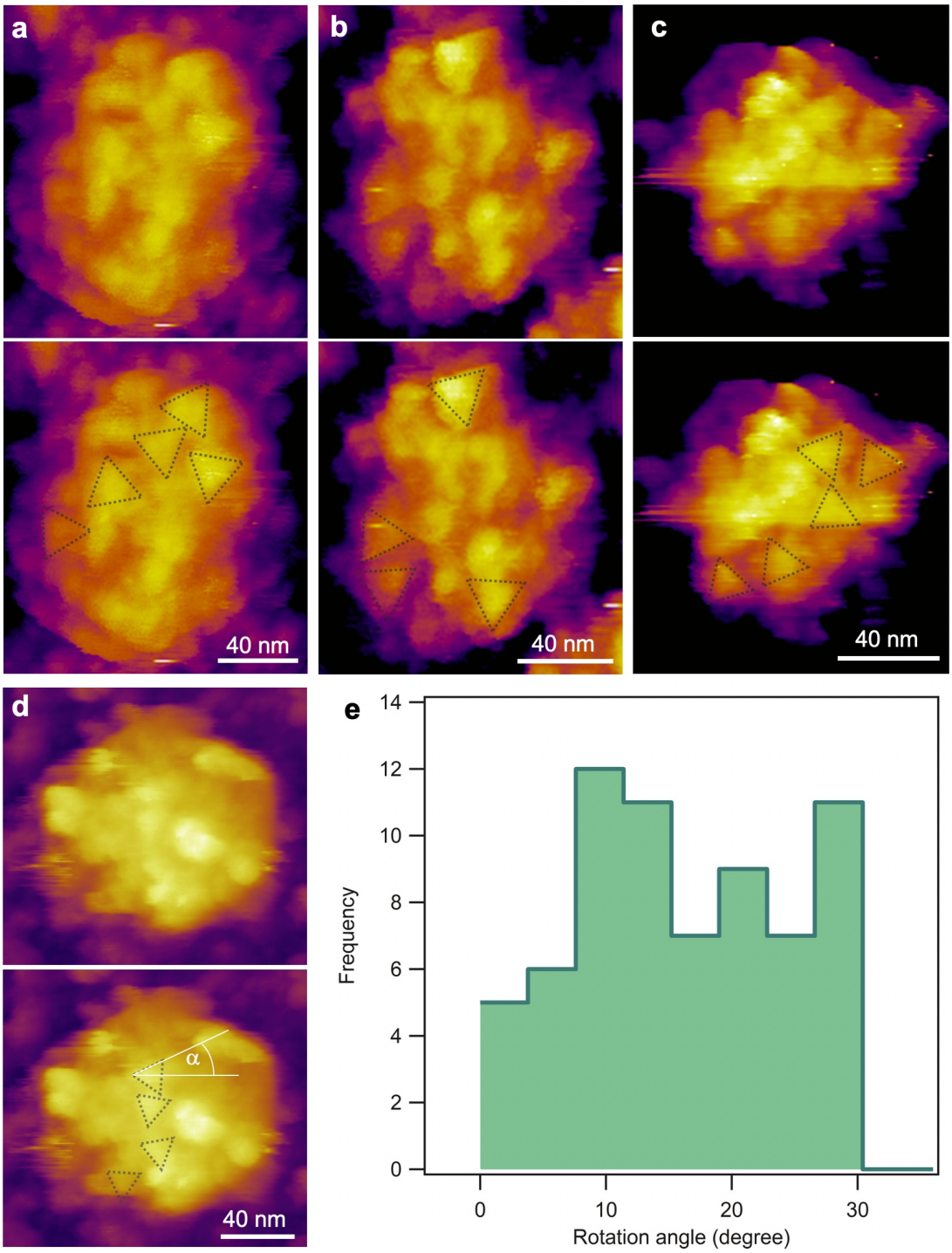

Fig. S4. Analysis of S-trimer rotational position. **a-c.** Examples of height-contrast AFM images of SARS-CoV-2 virus particles on the surface of which triangle-shape spikes can be identified. The upper figures show raw images, while in the lower ones equilateral triangles with dotted-line edges guide the visual identification of the triangular S-trimers. **d.** Principle of angle measurement. Height-contrast image of a SARS-CoV-2 virus particle (upper image). The lower image shows the same particle with equilateral triangles superimposed in the

putative S-trimers. The rotational position of the S-trimer was obtained by measuring the angle (α) between a horizontal reference line and the side of the triangle which was estimated to be closest to the horizontal. **b.** Distribution of rotational angles (n=68, range=30˚). In repeated scans of the same virus particle the orientation of a given S-trimer did not change. The different angles observed within a single image exclude the possibility that triangular appearance was caused by AFM tip artifact. The continuous distribution of rotational angles in our data suggest that there is large degree of rotational disorder, hence rotational freedom, associated with the spikes.

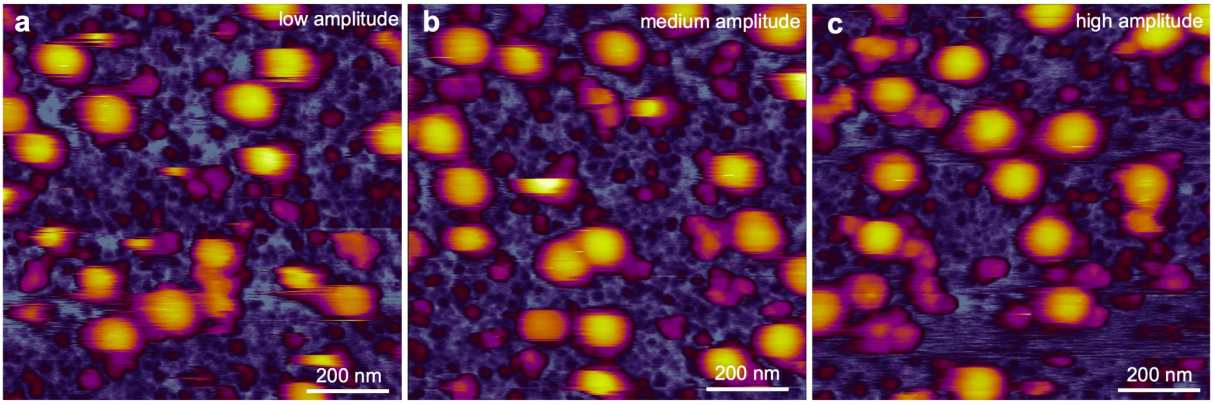

Fig. S5. Effect of cantilever oscillation amplitude on imaging native, unfixed SARS-CoV-2 virions. Setpoint per free-amplitude values were 120 mV/155 mV (**a**), 210 mV/280 mV (**b**) and 385 mV/500 mV (**c**).

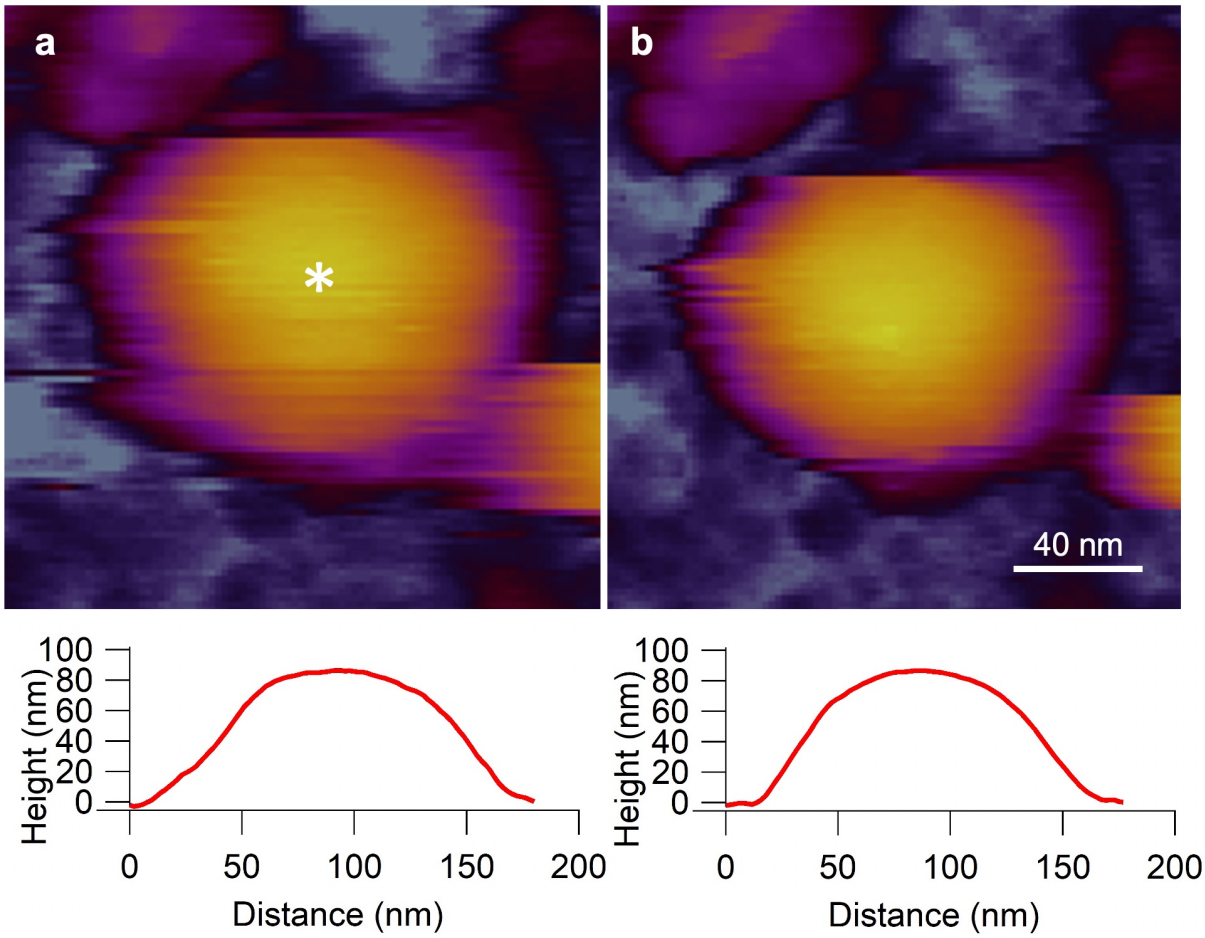

Fig. S6. Magnified view of the effect of nanoindentation on the native SARS-CoV-2 virion. Height contrast images of a SARS-CoV-2 virus particle prior to (**a**) and following (**b**) nanomechanical manipulation by the AFM tip. The exact tip location is shown with an asterisk. The plots below show topographical height profiles along horizontal diameters of the particles.

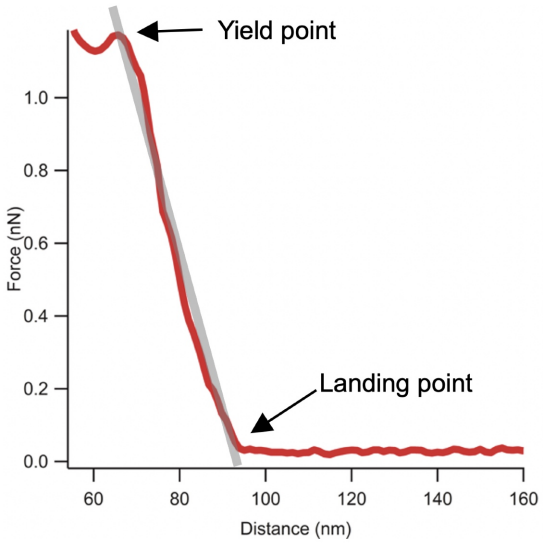

Fig. S7. Enlarged view of the indentation force curve to reveal the mechanical events immediately following the AFM tip landing on the virion surface and prior to mechanical yield. The grey line is a linear fit to this force range. The force data indicate that the SARS-CoV-2 virus particle follows Hookean elastic behavior in this regime with a single characteristic stiffness. The lack of discrete changes in the slope suggest that the spike layer does not contribute to the apparent mechanical behavior.

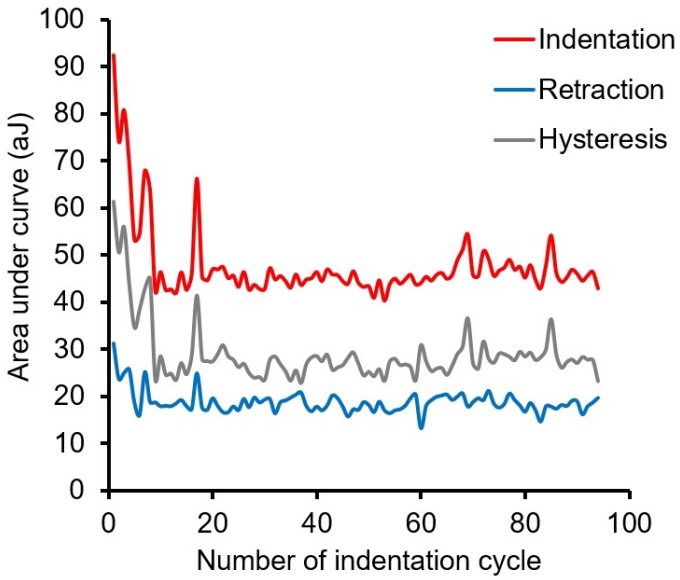

Fig. S8. Area under the indentation (red) and retraction (blue) curves and of the mechanical hysteresis (grey) as a function of the number of indentation cycle during successive nanomechanical manipulation of a SARS-CoV-2 virus particle. Area of hysteresis was calculated as the difference between the areas under the indentation and retraction force traces.

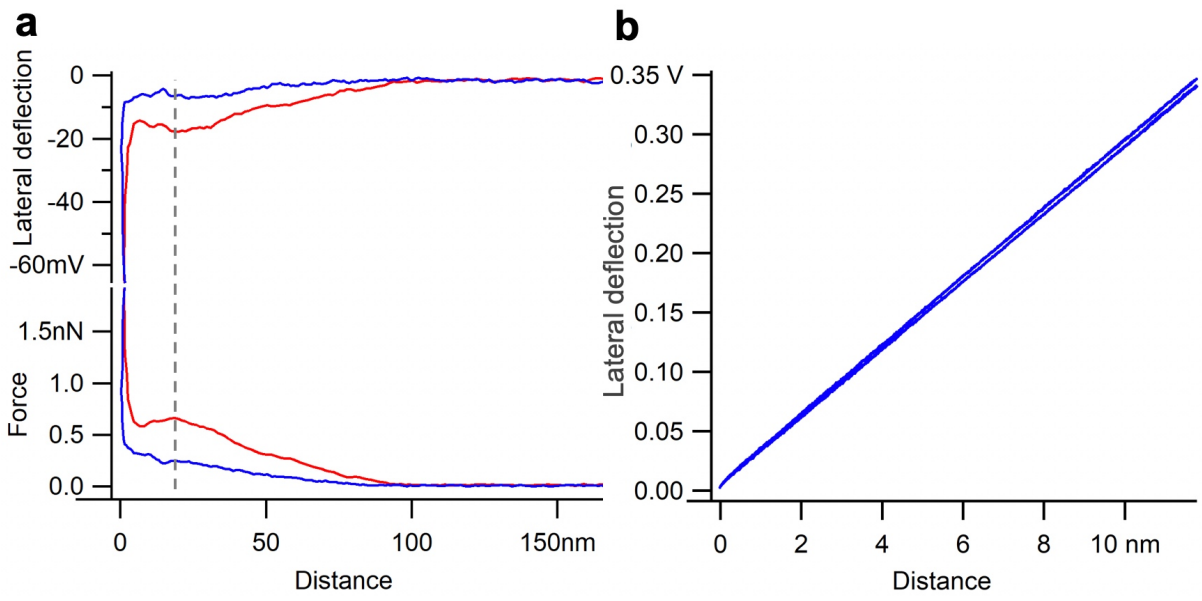

Fig. S9. Testing the contribution of cantilever torsion to the force spectrum. **a.** Force (in nN) and lateral displacement signal (in mV) as a function of distance obtained during an indentation-retraction experiment on a single SARS-CoV-2 virion. **b.** Calibration of lateral displacement. Lateral displacement (in volts) as a function of distance is shown. The trace was obtained in an experiment in which the cantilever was pressed, with a force of 2 nN, into a mica surface so as to immobilize the tip, then the cantilever was moved laterally (along a direction perpendicular to its long axis) with an amplitude of 10 nm. The nearly overlapping blue traces correspond to data acquired during back-and-forth motion. Such an experiment resulted in the torsion of the cantilever and provided means to measure the signal (volts) per unit torsional displacement (nm). From the slope of the line (29 mV/nm) we obtained the lateral distance calibration. The calibration indicated that the 19 mV lateral displacement signal measured at the 0.7 nN indentation force (gray dotted line in **a**) corresponds to a lateral distance of only 6.5 Å. Because this small distance is negligible in comparison to the virion diameter (<1 %), we exclude the possibility that during indentation the cantilever slips sideways off the virus particle.

SUPPLEMENTARY TABLES

Table S1. Particle analysis results. Particle height was measured in the center of particles. We used the mean height of the native virion (d_v) to calculate its mean surface area (A_v) as $d_v^2\pi$ = 21642 nm^2.

	Height (nm)	Volume (nm^3)	Diameter (nm)	n
Fixed	62 ± 8	574 000 ± 212 000	120 ± 16	51
Native	83 ± 7	490 000 ± 107 000	99 ± 11 nm	47
Heated (90 ˚C)	82 ± 10	600 000 ± 152 000	108 ± 12	37

Table S2. Spike analysis results. We assume that each spike occupies a circular area on the virion surface the diameter (d_s) of which is the mean nearest-neighbor distance. Hence, the mean area occupied by a spike is $(d_s/2)^2\pi$ = 356 nm^2. The ratio of the virion and spike-occupancy surfaces provides the average number of spikes on a virion: ~61.

	Mean ± S.D. (nm)	n
Nearest-neighbor distance	21 ± 6	197
Spike height	13 ± 5	80

Table S3. Structural and nanomechanical data extracted from force spectroscopy results.

	Height (nm)	Stiffness (pN/nm)	n
Native virion	94 ± 10	13 ± 5	40

EXPERIMENTAL DETAILS

Sample preparation

SARS-CoV-2 was isolated from the oropharyngeal swab of a laboratory-confirmed COVID-19 patient in Hungary and passed two times in VeroE6 cell line (European Collection of Authenticated Cell Culture, Salisbury, U.K.) in Dulbecco′s Modified Eagle′s Medium (Lonza, Basel, Switzerland) supplemented with 5% fetal bovine serum (EuroClone, Pero, Italy) and Cell Culture Guard (PanReac AppliChem, Darmstadt, Germany). To remove the disturbing effects of fetal bovine serum albumin, an additional passage was carried out in VP-SFM serum-free, ultra-low protein medium (Gibco, ThermoFisher Scientific) supplemented with L-glutamine (Sigma-Aldrich, Merck, Darmstadt, Germany). Four days after inoculation, when full cytopathic effects were observed, the virus-containing medium was collected and centrifuged (3000 x g) to remove debris. To concentrate the virus, the supernatant was ultracentrifuged (70,000 x g, 1.5 hours, 4°C) in 13.5-ml lockable plastic tubes using a Sorvall MTX-150 ultracentrifuge. The supernatant was removed and the pellet was resuspended in 100 µl VP-SFM. All sample preparation steps were performed in biosafety level-3 (BSL-3) conditions.

Preparation of affinity-enhanced substrate surface

100 µl of 0.1% w/v poly-L-lysine (PLL) (Merck, Darmstadt, Germany) solution was pipetted onto a freshly cleaved mica surface (Ted Pella, Redding, CA) and incubated for 20 minutes, following which the surface was rinsed with distilled water and dried in N_2 stream. 100 µl of 25% w/v grade I glutaraldehyde (GA) (Merck, Darmstadt, Germany) was then pipetted on the surface and incubated for 30 min, followed by further rinsing with distilled water and drying in N_2 stream. Subsequently, 100 µl of 10 µg/ml recombinant protein G (Merck, Darmstadt, Germany) was added and incubated for 30 minutes, then the surface was washed five times each with 100 µl phosphate-buffered saline (PBS). 100 µl of 10 µg/ml SARS-CoV-2 Spike Glycoprotein Antibody (#abx376478, Abbexa Ltd, Cambridge, UK) was then added, and the surface was incubated for 1 hour. All surface functionalization steps were performed at room temperature. Unbound antibodies were removed by repeated rinsing with PBS. The anti-spike glycoprotein antibody-coated surfaces were stored under PBS for up to 5 days at 4 °C.

Handling virion sample in the AFM

An aliquot (20 µl) of purified SARS-CoV-2 sample was pipetted onto the anti-spike antibody-coated substrate surface and incubated at 37 ˚C for 30 minutes. To increase virion surface

density, another aliquot was added and incubated. The process was repeated twice. Subsequently, the surface was rinsed gently with PBS to remove unbound virions. All the sample-loading and washing steps were carried out in a laminar-flow hood in BSL-3 conditions (at the National Biosafety Laboratory, National Public Health Center, Hungary). For AFM imaging of chemically fixed SARS-CoV-2, 100 µl 5% GA solution (in PBS) was added, and the sample was incubated for >1 hour, ensuring both fixation and virus inactivation. Then, the sample was carried to the AFM laboratory (Department of Biophysics and Radiation Biology, Semmelweis University) for loading in the environmental scanner unit of the Cypher ES AFM instrument. For imaging native virions, the fixation step was omitted and the sample was loaded directly in the Cypher ES Scanner. To ensure compliance with safety measures, a closed cantilever holder and gas-tight sample chamber was used, and the sample was loaded into the scanner in a laminar-flow hood in BSL-3 conditions. Then the scanner was carried to the AFM laboratory and inserted into the AFM instrument for imaging. To further comply with safety measures, following AFM imaging the native virus samples were discarded in either of two ways. In the first, the AFM scanner was taken to the BSL-3 laboratory for removal and chemical desctruction of the sample. In the second, the sample was heated to 90 ˚C for >10 minutes with the temperature-controller unit of the Cypher ES scanner. Then, the sample was removed for immediate chemical destruction (5% NaClO).

AFM imaging and force spectroscopy

Atomic force microscopy imaging was carried out with an Asylum Research Cypher ES instrument (Oxford Instruments, Santa Barbara, CA) [1, 2]. Resonant-mode (AC- or non-contact mode) scanning was performed under liquid in PBS with BL-AC40TS (Olympus Corporation, Japan) cantilevers. The cantilever was oscillated near its resonance frequency (tyically around 20 kHz) by using photothermal excitation at a typical free amplitude of 0.5 V. Imaging was carried out at a typical setpoint of 350 mV and with scanning speeds <1 µm/s to prevent the mechanical dislodging of virions from the substrate surface. Alternatively, we used fast force mapping (FFM, or "jumping-mode" AFM [3]) to collect image data. In FFM the cantilever was driven sinusoidally with a typical frequency of 300 Hz and a setpoint force of 100 pN to obtain a force curve for each pixel, from which the topographical image was reconstructed. The two (AC-mode and FFM) imaging modes gave similar results. Thermal exposure of the virions was achieved by heating the sample stage to pre-set temperatures[4]. Force spectroscopic measurements were carried out on virions selected on the AFM images. The cantilever was lowered, in contact mode, onto the vertex of the virion with 0.5 µm/s velocity until the setpoint

force was reached (typically 2-3 nN). Cantilever spring constants were determined by the thermal method[5] prior to imaging. Spring constants were between 90-120 pN/nm.

Data analysis

Image postprocessing and data analysis were performed by using the AFM driving software AR16, IgorPro 6.37 (Wavemetrics, Lake Oswego, OR). Particle analysis was carried out in subsequent analytical steps. First, the particles were demarcated by masking at the full width at half maximal height. Second, the mask was eroded, then dilated to gently smooth particle edges, while also getting rid of small scanning artefacts. We ignored particles with extreme deformities, ones too close to each other or with an area smaller than 3000 nm^2. Height was calculated at the center of the particles. Volume was calculated as the sum of the heights of individual pixels of the particle multiplied by the spatial (x, y) scaling values to correct for image pixel resolution. Particle diameter was calculated as the diameter of a circle with the same area as the particle itself.

REFERENCES

1. Kellermayer, M. S. Z.; Voros, Z.; Csik, G.; Herenyi, L. Forced phage uncorking: viral DNA ejection triggered by a mechanically sensitive switch. *Nanoscale* **2018,** 10, (4), 1898-1904.
2. Voros, Z.; Csik, G.; Herenyi, L.; Kellermayer, M. S. Stepwise reversible nanomechanical buckling in a viral capsid. *Nanoscale* **2017,** 9, (3), 1136-1143.
3. Moreno-Herrero, F.; Perez, M.; Baro, A. M.; Avila, J. Characterization by atomic force microscopy of Alzheimer paired helical filaments under physiological conditions. *Biophys J* **2004,** 86, (1 Pt 1), 517-25.
4. Voros, Z.; Csik, G.; Herenyi, L.; Kellermayer, M. Temperature-Dependent Nanomechanics and Topography of Bacteriophage T7. *J Virol* **2018,** 92, (20).
5. Hutter, J. L.; Bechhoefer, J. Calibration of atomic-force microscope tips. *Rev. Sci. Instrum.* **1993,** 64, (7), 1868-1873.